A WRF-Chem flash rate parameterization scheme and LNO_x analysis of the 29-30 May 2012 convective event in Oklahoma during DC3

Kristin Cummings[1,2,*], [1]Kenneth Pickering[3], Mary Barth[4], Megan Bela[5], Yunyao Li[1], Dale Allen[1], Eric Bruning[6], Don MacGorman[7], Steven Rutledge[8], Brody Fuchs[8], Andrew Weinheimer[4], Ilana Pollack[9], Thomas Ryerson[9], and Heidi Huntrieser[10]

1. University of Maryland, College Park, Maryland, U.S.A.
2. NASA Kennedy Space Center, Florida, U.S.A.
3. NASA Goddard Space Flight Center, Greenbelt, Maryland, U.S.A.
4. National Center for Atmospheric Research, Boulder, Colorado, U.S.A.
5. University of Colorado, Boulder, Colorado, U.S.A.
6. Texas Tech University, Lubbock, Texas, U.S.A.
7. NOAA/National Severe Storms Laboratory, Norman, Oklahoma, U.S.A.
8. Colorado State University, Fort Collins, Colorado, U.S.A.
9. NOAA CSD, Boulder, Colorado, U.S.A.
10. Institut für Physik der Atmosphäre, Deutsches Zentrum für Luft-und Raumfahrt, Oberpfaffenhofen, Germany

ABSTRACT: The Deep Convective Clouds and Chemistry (DC3) field campaign in 2012 provided a plethora of aircraft and ground-based observations (e.g., trace gases, lightning and radar) to study deep convective storms, their convective transport of trace gases, and associated lightning occurrence and production of nitrogen oxides (NO_x). Based on the measurements taken of the 29-30 May 2012 Oklahoma thunderstorm, an analysis against a Weather Research and Forecasting Chemistry (WRF-Chem) model simulation of the same event at 3-km horizontal resolution was performed. One of the main objectives was to include various flash rate parameterization schemes (FRPSs) in the model and identify which scheme(s) best captured the flash rates observed by the National Lightning Detection Network (NLDN) and Oklahoma Lightning Mapping Array (LMA). The comparison indicates how well the schemes predicted the timing, location, and number of lightning flashes. The FRPSs implemented in the model were based on the simulated thunderstorm's physical features, such as maximum vertical velocity, cloud top height, and updraft volume. Adjustment factors were applied to each FRPS to best capture the observed flash trend and a sensitivity study was performed to compare the range in model-simulated lightning-generated nitrogen oxides (LNO_x) generated by each FRPS over the storm's lifetime. Based on the best FRPS, model-simulated LNO_x was compared against aircraft measured NO_x. The trace gas analysis, along with the increased detail in the model specification of the vertical distribution of lightning flashes as suggested by the LMA data, provide guidance in determining the scenario of NO production per intracloud and cloud-to-ground flash that best matches the NO_x mixing ratios observed by the aircraft.

* Contact information: Kristin Cummings, University of Maryland, College Park, Maryland, U.S.A., Email: kristin@atmos.umd.edu

INTRODUCTION

Obtaining a better understanding of deep convective clouds is important for expanding our knowledge of the atmosphere and for correctly capturing critical processes, such as convective transport, lightning flash rate trends, and lightning-generated nitrogen oxides (LNO_x). Each process, especially lightning related chemistry, contains some degree of uncertainty and needs to be properly understood for their inclusion in climate models.

In the troposphere, the nitrogen oxide ($NO_x = NO + NO_2$) budget is comprised of both natural and anthropogenic sources. The major processes involved in NO_x emissions include fossil fuel combustion, biomass burning, microbial activity in soils, and lightning [Schumann and Huntrieser, 2007]. The lower troposphere is mainly dominated by surface emissions, especially those due to human activities [Zhang et al., 2003]. Lightning is one of the largest natural sources, accounting for roughly 5±3 Tg (N) yr^{-1}, or 10-15%, of the total NO_x budget [Schumann and Huntrieser, 2007]. More importantly, lightning is the largest source of NO_x in the upper troposphere. Most LNO_x is present above an altitude of 7 km [Martin et al., 2007], where the lifetime of NO_x is longer and has implications for indirectly affecting the climate via ozone (O_3) production. Following a convective event, enhancements in O_3 can be found downwind within the thunderstorm outflow [DeCaria et al., 2005; Ott et al., 2010; Martini et al., 2011], resulting from photochemistry involving NO_x. The enhancements in O_3 increase its radiative forcing, which maximizes near the tropopause, and raises the possibility of a positive feedback between lightning and temperature. Nitrogen oxides are also important because they affect the hydroxyl radical (OH) concentration, which is known as the "detergent of the atmosphere" because of its ability to react with and remove various trace gas species (e.g., CO, SO_2, NO_2, and hydrocarbons) from the atmosphere.

Many factors affect the uncertainty of LNO_x production, including the location and strength of the convection and the type, length, and energy of the lightning flash. Although other natural and anthropogenic NO_x sources may have uncertainty ranges that are similar to or greater than that associated with lightning, the potential positive feedback mechanism between lightning and surface temperatures makes narrowing the uncertainty range of LNO_x critical [Schumann and Huntrieser, 2007]. In addition, a better understanding of the global LNO_x budget would be beneficial for properly modeling variations and trends in NO_x and O_3 and in analyzing the influence of other NO_x sources, such as the injection of stratospheric NO_x and aircraft emissions [Zhang et al. 2000; Bond et al., 2001].

To further address how LNO_x and other trace gases are influenced by convective transport and lightning flash rates, cloud-resolved model simulations of observed storms will be run using observed flashes and those predicted using storm features (e.g., cloud top height and maximum vertical velocity). The Deep Convective Clouds and Chemistry (DC3) field campaign in May-June 2012 focused on thunderstorms in northeast Colorado, central Oklahoma, and northern Alabama. The purpose of the campaign was to study varying types of convection (e.g., midlatitude airmass, multicell, and supercell thunderstorms), their convective transport of trace gases (e.g., anthropogenic, biogenic, and wildfire emissions), and associated lightning occurrence and NO_x production. Based on the extensive ground-based and aircraft observations (e.g., trace gases, lightning, and radar) collected during the campaign, cloud-resolved model simulations are evaluated to

determine how well storm features and observed measurements were reproduced, and if representation of storm characteristics, such as lightning flash rate and NO production scenarios, need adjustment for use in future climate models. This analysis focuses on the 29-30 May 2012 Oklahoma thunderstorm observed during DC3.

BACKGROUND

Lightning instrumentation

One reason central Oklahoma was selected as a domain for thunderstorm observation is due to its extensive network of lightning measurements. Two-dimensional (2D) ground-based observations are available from the National Lightning Detection Network (NLDN). More than 100 sensors make up the network, which uses magnetic direction finding and time-of-arrival techniques to map sources of the low frequency (LF) and very low frequency (VLF) emissions released by CG flashes occurring over the continental United States and over nearby coastal regions [LaJoie and Laing, 2008; Orville, 2008; Vaisala, 2014]. The information in the dataset includes the time and location of the flash, as well as its polarity, strength, the number of return strokes (multiplicity), 50% location error ellipse data, and several other parameters. The NLDN observes some fraction of IC flashes, but with lower detection efficiency (DE). A rough estimate of the total number of lightning flashes may be obtained from the NLDN CG flash data using:

$$total\ flashes = CG\ flashes \times \frac{1}{NLDN\ DE} \times [IC{:}\,CG\ ratio\ + 1] \qquad (1)$$

where the NLDN DE currently equals ~93% and the ratio of IC to CG flashes may be based on the spatially-varying climatological mean IC:CG ratios over the United States [Boccippio et al., 2001].

Three-dimensional (3D) systems, called lightning mapping arrays (LMAs), are also available in several locations across the United States, including Oklahoma/west Texas. Figure 1 indicates the location of the LMA stations and the extent of the 2D and 3D coverage of the Oklahoma/west Texas network. The 3D systems, developed by New Mexico Tech (NMT), include multiple stations, which use time-of-arrival sensors to detect the very high frequency (VHF) electromagnetic pulses emitted by a lightning flash. The result is a 3D map of total lightning activity, although the sensors mainly detect IC flashes and the mid-to-upper level segments of CG flashes [Stano et al., 2010]. The LMA DE is effectively 100% over the network and within a 75-100 km range from the network center; however, there is a large decrease in DE outside the 200 km range. After data processing, the NMT LMAs can provide the following types of data at various temporal and spatial resolutions: VHF source density, flash extent density, flash initiation density, and average flash area.

Flash rate parameterization schemes

Lightning flash rate time series are helpful when investigating the influence of LNO_x on the chemistry within and downwind of a thunderstorm. However, in instances when lightning observations are not available for incorporation into a model-simulated thunderstorm, flash rate parameterization schemes (FRPSs) are an option.

Cloud-resolving models have previously incorporated explicit electrical schemes to study lightning activity in thunderstorms (e.g., Ziegler and MacGorman, 1994; Mansell et al., 2002; Barthe et al., 2005). The difficulty with using explicit schemes for simulating lightning flashes is not only the complexity of the electrical activity, but also the cost to model the intricate behavior [McCaul et al., 2009]. To avoid these difficulties, use of FRPSs based on storm parameters already available in models is a useful way to simulate a thunderstorm's electrical activity.

Relationships between ice-phase hydrometeors and lightning have previously been used in cloud-resolved models to predict total lightning flashes. Ice water path [Petersen et al., 2005], ice mass flux product, and precipitation ice mass [Deierling et al., 2008] are examples of flash rate-storm parameter relationships involving hydrometeors. McCaul et al. [2009] developed several methods for forecasting flash rates using graupel and vertically integrated ice based on selected convective events over Northern Alabama. These two methods capture different aspects of the lightning activity, such as temporal variability and areal coverage, respectively. However, a combination of the two methods provides a better flash rate prediction over the case study region. Previous research has also investigated correlations between lightning and non-hydrometeor parameters. These parameters include maximum vertical velocity, cloud top height [Price and Rind, 1992], and updraft volume [Deierling and Petersen, 2008].

Six (of nine) types of FRPSs were evaluated with the Weather Research and Forecasting (WRF) model at cloud-resolved scales (Table 1). Barthe et al. [2010] simulated an isolated severe storm observed during the Stratosphere-Troposphere Experiment: Radiation, Aerosols, and Ozone (STERAO-A) and an airmass thunderstorm over northern Alabama. Their research differs from previous work because it was the first time field experiment observations were used to create flash rate-storm parameter relationships, which were tested in a model. Cummings et al. [2013] used the WRF Aqueous Chemistry (WRF-AqChem) model to simulate a deep convective thunderstorm, which occurred during the Stratospheric-Climate Links with Emphasis on the Upper Troposphere and Lower Stratosphere (SCOUT-O3)/Aerosol and Chemical Transport in Tropical Convection (ACTIVE) field campaigns near Darwin, Australia. Further research by Cummings [2013] represents the first simulation of tropical island convection using FRPSs.

Lightning-generated nitrogen oxides

A lightning flash is brief, but its high temperature partly dissociates molecular oxygen (O_2) and nitrogen (N_2), which allows oxygen and nitrogen atoms to react and produce nitric oxide (NO). The lifetime of NO_x varies as a function of altitude, with lifetimes on the order of a day or less near the earth's surface to lifetimes as long as several days to a week in the upper troposphere [Ridley et al., 1996; Huntrieser et al., 1998; Jaeglé et al., 1998; Martin et al., 2007]. The variation is mainly due to two mechanisms involving the production of HNO_3. The reaction between nitrogen dioxide (NO_2) and OH to make HNO_3 is temperature dependent, so the reaction rate slows as the temperature decreases with altitude between the surface and the tropopause. Nitrogen dioxide is also involved in the production of N_2O_5. However, the heterogeneous production of HNO_3 slows because the reaction between N_2O_5 and water occurs on aerosols, which there are fewer of in the upper troposphere. There is also a greater

tendency for NO_x to exist as NO [Jaeglé et al., 1998] in the upper troposphere due to other temperature dependent reactions that slow with altitude, such as those between NO and O_3 and between NO and HO_2.

Unfortunately, direct measurements of the global LNO_x budget are not possible, although cloud-resolving models and observations from satellites and aircraft have helped to slightly reduce the uncertainty. The best approximation for the contribution of lightning to the global NO_x budget is 5±3 Tg (N) yr^{-1} [Schumann and Huntrieser, 2007]. The main areas of uncertainty include the production of NO per IC and CG flashes, the amount of NO produced per unit flash length, and the vertical profile of LNO_x mass [Ott et al., 2010]. Analyses investigating types and lengths of lightning flashes indicate the amount of NO produced per meter flash channel length is less in IC versus CG flashes and that longer flash lengths produce more LNO_x [Barthe and Barth, 2008; Huntrieser et al., 2008]. However, other cloud-resolved modeling constrained by aircraft observations [DeCaria et al., 2000; 2005, Ott et al., 2010] suggests that on average IC and CG flashes make similar amounts of NO.

For a "typical" thunderstorm the accepted LNO_x production range is 33-660 moles NO $flash^{-1}$, with an average production rate of 250 moles NO $flash^{-1}$ [Schumann and Huntrieser, 2007]. Previous analyses of midlatitude thunderstorms suggest 200-500 moles NO $flash^{-1}$ is a reasonable estimate [DeCaria et al., 2000, 2005; Fehr et al., 2004; Ott et al., 2007]. Five convective events taken from the midlatitudes and subtropics also found a mean value of 500 moles NO $flash^{-1}$ [Ott et al., 2010]. A Hector thunderstorm simulation indicated a NO production scenario of 500 moles $flash^{-1}$ was representative of tropical island convection; however, 600 moles NO $flash^{-1}$ was not unreasonable as an upper limit [Cummings et al., 2013]. Although the LNO_x production from each of these analyses falls within the range of a "typical" thunderstorm, the variation indicates uncertainty still exists. In addition, Ott et al. [2010] suggest the amount of LNO_x per unit flash length ranges from 1.7 to 22 x 10^{-3} moles NO m^{-1} due to the influence of peak current and ambient pressure. Despite the difficulties related to making direct LNO_x measurements, researchers would like to decrease the uncertainty range of the global LNO_x budget to ±1 Tg (N) yr^{-1} or 20% [Schumann and Huntrieser, 2007].

WRF-CHEM MODEL

The 3D WRF model coupled with Chemistry (WRF-Chem) is a cloud-resolving model, which combines the mesoscale forecasting capabilities of the WRF model with chemistry modeling [Grell et al., 2005]. The WRF-Chem allows for online simulations, which more accurately characterize the production and transport of trace gases and aerosols and guarantees consistency with the meteorological fields. A WRF-Chem model simulation of the observed 29-30 May thunderstorm was performed for this analysis using a two-way nested grid. The horizontal resolutions were 15-km and 3-km for the parent and inner domains, respectively. The focus of this analysis is on the inner domain, which contains 280 and 340 grid points in the east-west and north-south direction, respectively. There are 39 grid points in the vertical direction, with the mean vertical grid spacing stretching from 59 m at the surface to 1005 m at the top of the domain, which is 20.2 km. The simulation was initialized and constrained by the meteorological conditions provided by the Global Forecasting System (GFS). The Model for Ozone And Related chemical Tracers version 4 (MOZART) is an offline global chemical tranport

model, which is suited for the troposphere [Emmons et al., 2010]. The output from MOZART generated the chemical initial and boundary conditions for WRF-Chem.

The physical and chemical processes represented in the WRF-Chem include transport, deposition, anthropogenic and biogenic emissions, gas-phase chemical transformation, aerosol interactions, photolysis, and radiation [Grell et al., 2005]. The Morrison 2-moment microphysics scheme was selected for the initial set-up of the WRF-Chem. This scheme is an advanced double-moment scheme, which includes five hydrometeor species with the mass mixing ratios and number concentrations determined for each [Morrison et al., 2009]. The Mellor-Yamada-Janjic (MYJ) planetary boundary layer (PBL) scheme was also incorporated, along with the Grell-3D (G3) cumulus scheme, which was used in the parent domain for its compatibility with chemistry.

The chemical processes are provided by the MOZART chemistry scheme, which is connected to WRF-Chem via the Kinetic PreProcessor (KPP). The chemical mechanism contains gas-phase species, bulk aerosol compounds, and photolysis and gas-phase reactions, in addition to an updated isoprene oxidation scheme and a separation of volatile organic compounds into three groups (i.e., alkanes, alkenes, and aromatics). The Georgia Tech/Goddard Chemistry Aerosol Radiation and Transport (GOCART) model is a bulk aerosol scheme, which determines the total mass of each aerosol type, but does not provide particle size information, except for dust and sea salt [Chin et al., 2000]. This scheme is considered numerically efficient and allows for simulations with complex gas-phase and aqueous chemistry. The GOCART aerosol scheme was combined with the MOZART chemical scheme (MOZCART) for use in WRF-Chem.

Lightning-generated nitrogen oxides parameterization schemes

The LNO_x production in WRF-Chem may be estimated for both cloud-resolved and parameterized convection given the lightning flash rate time series, the horizontal and vertical distribution of lightning flashes, and the NO production per IC and CG flashes are provided. Flash rates can either be predicted from storm parameters or, to reduce uncertainty, prescribed directly from lightning observations [DeCaria et al., 2005; Ott et al., 2010; Cummings et al., 2013]. Likewise, the flash type can be predicted [Price and Rind, 1993; Pickering et al., 1998; Fehr et al., 2004] or prescribed from observations [DeCaria et al., 2005; Ott et al., 2007, 2010].

The vertical distribution of LNO_x may be specified in WRF-Chem following two methods. The first approach is used in a cloud-resolved domain and assumes the vertical distribution of NO_x follows the Gaussian distributions representative of typical CG (unimodal) and IC (bimodal) lightning flash channel segments (Fig. 2) [DeCaria et al., 2000, 2005]. The lightning channels are set to maximize at specified lower (CG and IC flashes) and upper (IC flashes) temperature levels, which may be adjusted for higher or lower cloud tops. For midlatitude thunderstorms, the channels are set to -15°C and -45°C. The second approach is appropriate for WRF-Chem model simulations performed with parameterized convection. This method provides the vertical distributions of LNO_x resulting from both production and convective transport [Pickering et al., 1998; Ott et al., 2010].

At each horizontal layer in the model, the NO_x is placed uniformly into each grid cell within the convective cloud where radar reflectivities $\geq$ 20 dBZ. The NO production per flash scenarios for IC and CG flashes vary by each type of thunderstorm simulation.

The initial assumption for midlatitude convection is usually 500 moles NO per IC and CG flashes [Ott et al., 2010]. The NO production scenarios per flash type are adjusted as needed if anvil comparisons between the model and aircraft observations indicate the anvil NO_x mixing ratios are not similar.

During the DC3 field campaign, the DeCaria et al. [2000] LNO_x parameterization scheme was implemented in the WRF model, in conjunction with the updraft volume FRPS, to forecast the amount and location of the LNO_x tracer. In the near future, the DeCaria et al. [2000] LNO_x parameterization scheme may be updated with new vertical distributions of lightning channels for each of the DC3 domains (i.e., northeast Colorado, Oklahoma/west Texas, and northern Alabama). The distributions will be produced by Colorado State University (CSU), Texas Tech University (TTU), or the University of Alabama Huntsville (UAH)/NASA Marshall Space Flight Center (MSFC) using LMA data from their own domain.

THE 29-30 MAY 2012 OKLAHOMA CONVECTIVE EVENT

On the morning of 29 May 2012 conditions were very unstable and favorable for convective development within the Oklahoma domain. The synoptic-scale analysis (Fig. 3) at 12:00 UTC showed a cold front stretching across the Ohio River Valley from northeast-to-southwest, with the southern portion pushing northward as a warm front over Oklahoma and Kansas. A dryline was also set-up across the Texas Panhandle. Around 23:00 UTC the upper level winds were generally from the west with veering from the surface to 700 mb (Fig. 4). Figure 4 also indicates the sounding had a convective available potential energy (CAPE) value of 3440 J kg^{-1}. During the afternoon, New Mexico wildfire plumes were expected to reach the southwestern edge of the Oklahoma/west Texas domain in the lower troposphere.

The observed thunderstorm developed along the Kansas/Oklahoma border around 21:00 UTC, ahead of the dryline and south of the warm front. The storm system continued in an east-southeast direction, merging with other cells to form a MCS, and dissipated around 04:00 UTC on 30 May. The NASA DC-8 focused on storm inflow and outflow, while the NSF/NCAR Gulfstream-V (GV) and DLR Falcon concentrated on high-altitude outflow. The National Severe Storms Laboratory (NSSL) also performed three mobile soundings in the vicinity of the storm. The NLDN CG flash data is provided at 1-min intervals and converted to total flashes (Eqn. 1). Figure 5 shows the movement of the storm and its associated CG lightning flashes. A climatological mean IC:CG ratio (3.9 ± 0.49) was also calculated for the storm region based on monthly gridded data files resulting from the analysis of Boccippio et al. [2001]. Flash initiation density data from the Oklahoma LMA was provided on a 3-km horizontal resolution grid at 5-min intervals and is summed over space and time to get a total flash count.

Total lightning flashes from the NLDN and Oklahoma LMA have not yet been incorporated into the model. Instead, the FRPSs (Table 1), which best capture the flash rates observed by the NLDN and Oklahoma LMA, were included in the model. To isolate the observed storm system, 10-min moving spatial masks were manually generated based on NEXRAD composite radar reflectivity, satellite observations, and observed flash rate time series plots. The procedure was repeated for the model-simulated storm, except the masks were based on the composite radar reflectivity and total hydrometeors output by the model.

The model-simulated cell began 1-1.5 h earlier (20:00 UTC) than the observed storm system, but in a similar location along the Kansas/Oklahoma border. As the simulated storm evolves, its area, based on composite reflectivity and total condensate, generally exceeds the area of the observed storm by roughly a factor of two (Fig. 6).

Meteorological analysis

One of the main objectives of this case study is to utilize six (of nine) FRPSs in the model and identify which scheme(s) best captures the observed total lightning flash rates. The WRF-Chem instantaneous flash rates at 10-min intervals were compared with the corresponding 1-min periods from the observed NLDN flash rates in an offline calculation. The offline calculation gives a best guess as to which FRPS(s) should be run online in the model, which is both a cost and time saver. Table 2 shows the scaling factors applied to each FRPS in the offline calculation and indicates the maximum vertical velocity and ice water path schemes need the least adjustment to match the observed total flashes at each 10-minute interval.

There is about a 20-min lag between when storm development is first indicated by the NEXRAD composite reflectivity (~21:00 UTC) and when the initial lightning flashes are detected. Several of the FRPSs (i.e., precipitation ice mass and ice mass flux product) show roughly a 40-min delay from when the simulated storm began (20:00 UTC) to the first model-simulated flashes, while the other schemes indicate flashes start at or before the model thunderstorm was indicated by composite reflectivity. Since the FRPSs are based on storm parameters already available in the model, lightning flashes will begin as soon as the conditions required for using the FRPSs are met. Figure 7 compares the NLDN observed and model-simulated flash rate trends, where the FRPS output has been shifted later by 90 minutes to account for the model convection's earlier start. The increasing trend of the observed flash rates is reproduced fairly well by the updraft volume, ice mass flux product, and precipitation ice mass schemes. Cloud top height generally captures the first four hours of the NLDN flash rate trend, but it misses the primary peak and initially over predicts the observed flashes. Maximum vertical velocity and ice water path also fail to capture the observed primary peak; however, both schemes mimic several NLDN flash rate peaks (22:20 UTC, 23:20 UTC, 01:10 UTC). None of the FRPSs contained a primary peak with the same magnitude as the observations (~430 flashes min^{-1}).

Based on the offline calculations, the maximum vertical velocity scheme was selected to be used in the model. This FRPS required little adjustment to match the observed total flashes and several of its flash rate peaks coincided with peaks in the observations. The model-simulated IC and CG flash counts are provided at 10-min intervals, with a storm total of 112,601 flashes (Fig. 8). However, the model run currently ends before the simulated storm dissipates, which suggests the number of model-simulated total flashes will likely be higher. Compared with the total lightning observations from the NLDN (45,751) and LMA (31,553), maximum vertical velocity overestimates the flashes detected by both networks by a factor of ~2.5 and ~3.5, respectively. Detection efficiency may be reduced over the northern edge of the LMA where the observed storm passes. This could partially explain the overestimation by the model. Also, given the area of the model-simulated storm is about doubled, simulated lightning may occur over a greater area than detected in the observed system. The

difference in total flashes between the offline and online calculations is due to the fact that in the offline calculation the NLDN data are compared with just the instantaneous 10-min interval storm parameter output.

Trace gas analysis

The DC-8 and GV sampled the cloud-free air to the south of the storm system to determine a baseline for the upper tropospheric background chemical environment. To define the background air at 9-12 km, the 10^{th} percentile is used to remove any influence from old convective outflow. The upper tropospheric flights by the aircraft indicate background NO_x values were around 0.06 parts per billion volume (ppbv; Fig. 9). Model-simulated NO_x mixing ratios (with no LNO_x) were compared against the observations at a similar time and location in the upper troposphere. The NO_x mixing ratios range from 0.05-0.5 ppbv in the model-simulation (Fig. 10). Although the observed NO_x is found at the lower end of this range, it should be kept in mind that the observed value represents the 10^{th} percentile. This indicates the initial WRF-Chem simulation of the 29-30 May thunderstorm appears to properly capture the aircraft measurements of the background air between 9-12 km.

The morning of the 29 May research flight the LNO_x WRF model tracer forecast for the Oklahoma convection predicted roughly 2-3 ppbv LNO_x in storm cores developing within the Oklahoma domain (Fig. 11). Within the anvils, the model forecasted about 1-2 ppbv NO_x due to lightning. The forecast provides an estimation of the LNO_x mixing ratios that may be observed by aircraft in the storm outflow at anvil height.

FUTURE SIMULATIONS AND ANALYSES

Future work includes running the current set-up of the WRF-Chem model (e.g., Morrison two-moment microphysics and MYJ PBL schemes) with the DeCaria et al. [2000, 2005] LNO_x parameterization scheme and comparing the aircraft observations against the model-simulated CO, NO_x, and O_3. The focus of the trace gas analysis will be on the model run which uses the FRPS(s) that best captures the observed total flash rates. However, each of the nine FRPSs will be run in the model, so the model-simulated LNO_x produced by each scheme may be compared against each other and the aircraft measured NO_x. We will also test new FRPSs developed from DC3 data by CSU, such as graupel echo volume, 30-dBZ echo volume, and updated versions of the nine current schemes. The observed lightning flashes will also be incorporated into the WRF-Chem to create another set of LNO_x output to compare with aircraft observations and the other model simulations. Overall, the LNO_x analysis will help identify the most appropriate NO production scenario for IC and CG flashes in the observed storm and establish if it is similar to other previously investigated midlatitude thunderstorms.

An investigation of the convective outflow plume downwind of the region sampled by the aircraft on the evening of 29 May is also planned. The model run time will be extended, so changes in trace gases, particularly O_3, may be analyzed downwind over southern Appalachia where the plume was located on 30 May by the aircraft.

ACKNOWLEDGMENTS

We would like to thank Cameron Homeyer (NCAR) for providing the regional NEXRAD level II data. NLDN data are collected by Vaisala, Inc. and archived by NASA MSFC.

REFERENCES

Barthe, C., and M. C. Barth, 2008: Evaluation of a new lightning-produced NO_x parameterization for cloud resolving models and its associated uncertainties, *Atmos. Chem. Phys.*, **8**, 4691-4710, doi:10.5194/acp-8-4691-2008.

Barthe, C., G. Molinié, and J.-P. Pinty, 2005: Description and first results of an explicit electrical scheme in a 3D cloud resolving model, *Atmos. Res.*, **76**, 95-113.

Barthe, C., W. Deierling, and M. C. Barth, 2010: Estimation of total lightning from various storm parameters: A cloud-resolving model study, *J. Geophys. Res.*, **115**, D24202, doi:10.1029/2010JD01445.

Bond, D. W., R. Zhang, X. Tie, G. Brasseur, G. Huffines, R. E. Orville, and D. J. Boccippio, 2001: NO_x production by lightning over the continental United States, *J. Geophys. Res.*, **106**, doi:10.1029/2000JD000191.

Chin, M., R. B. Rood, S.-J. Lin, J. F. Muller, and A. M. Thompson, 2000: Atmospheric sulfur cycle in the global model GOCART: Model description and global properties, *J. Geophys. Res.*, **105**, 24671-24687.

Cummings, K. A., 2013: Lightning flash rate and chemistry simulation of tropical island convection using a cloud-resolved model, M.S. scholarly paper, Department of Atmospheric and Oceanic Science, University of Maryland, College Park, Maryland, 72 pp.

Cummings, K. A., T. L. Huntemann, K. E. Pickering, M. C. Barth, W. C. Skamarock, H. Höller, H.-D. Betz, A. Volz-Thomas, H. and Schlager, 2013: Cloud-resolving chemistry simulation of a Hector thunderstorm, *Atmos. Chem. Phys.*, **13**, 2757-2777.

DeCaria, A. J., K. E. Pickering, G. L. Stenchikov, J. R. Scala, J. L. Stith, J. E. Dye, B. A. Ridley, and P. Laroche, 2000: A cloud-scale model study of lightning-generated NO_x in an individual thunderstorm during STERAO-A, *J. Geophys. Res.*, **105**, doi:10.1029/2000JD900033.

DeCaria, A. J., K. E. Pickering, G. L. Stenchikov, and L. E. Ott, 2005: Lightning-generated NO_x and its impact on tropospheric ozone production: A 3-D modeling study of a STERAO-A thunderstorm, *J. Geophys. Res.*, **110**, D14303, doi:10.1029/2004JD05556.

Deierling, W. and W. A. Petersen, 2008: Total lightning activity as an indicator of updraft characteristics, *J. Geophys. Res.*, **113**, D16210, doi:10.1029/2007JD009598.

Deierling, W., W. A. Petersen, J. Latham, S. Ellis, and H. J. Christian, 2008: The relationship between lightning activity and ice fluxes in thunderstorms, *J. Geophys. Res.*, **113**, D15210, doi:10.1029/2007JD009700.

Emmons, L. K., S. Watlers, P. G. Hess, J.-F. Lamarque, G. G. Pfister, D. Fillmore, C. Granier, A. Guenther, D. Kinnison, T. Laepple, J. Orlando, X. Tie, G. Tyndall, C. Wiedinmyer, S. L. Baughcum, and S. Kloster, 2010: Description and evaluation of the Model for Ozone and Related chemical Tracers, version 4 (MOZART-4), *Geosci. Model Dev.*, **3**, 43-67.

Fehr, T., H. Höller, and H. Huntrieser, 2004: Model study on production and transport of lightning-produced NO_x in a EULINOX supercell storm, *J. Geophys. Res.*, **109**, D09102, doi:10.1029/2003JD003935.

Grell, G. A., S. E. Peckham, R. Schmitz, S. A. McKeen, G. Frost, W. C. Skamarock, and B. Eder, 2005: Fully coupled "online" chemistry within the WRF model, *Atmos. Env.*, **39**, doi:10.1016/j.atmosenv.2005.04.027.

Huntrieser, H., H. Schlager, C. Feigl, and H. Höller, 1998: Transport and production of NO_x in electrified thunderstorms: Survey of previous studies and new observations at midlatitudes, *J. Geophys. Res.*, **103**, doi:10.1029/98JD02353.

Huntrieser, H., U. Schumann, H. Schlager, H. Höller, A. Giez, H.-D. Betz, D. Brunner, C. Forster, O. Pinto Jr., and R. Calheiros, 2008: Lightning activity in Brazilian thunderstorms during TROCCINOX: implications for NO_x production, *Atmos. Chem. Phys.*, **8**, 921-953, doi:10.5194/acp-8-921-2008.

Jaeglé, L., D. J. Jacob, Y. Wang, A. J. Weinheimer, B. A. Ridley, T. L. Campos, G. W. Sachse, and D. E. Hagen, 1998: Sources and chemistry of NO_x in the upper troposphere over the United States, *Geophys. Res. Lett.*, **25**, doi:10.1029/97GL03591.

LaJoie, M., and A. Laing, 2008: The influence of the El Niño-Southern Oscillation on cloud-to-ground lightning activity along the Gulf Coast. Part 1: Lightning climatology. *Mon. Wea. Rev.*, **136**, doi:10.1175/2007MWR2227.1.

Mansell, E. R., D. R. MacGorman, J. M. Straka, and C. L. Ziegler, 2002: Simulated three-dimensional branched lightning in a numerical thunderstorm model. *J. Geophys. Res.*, **107** (9), 4075, doi:10.1029/2000JD000244.

Martin, R. V., B. Sauvage, I. Folkins, C. E. Sioris, C. Boone, P. Bernath, and J. Ziemke,

2007: Space-based constraints on the production of nitric oxide by lightning, *J. Geophys. Res.*, **112**, doi:10.1029/2006JD007831.

Martini, M., D. J. Allen, K. E. Pickering, G. L. Stenchikov, A. Richter, E. J. Hyer, and C. J. Loughner, 2011: The impact of North American anthropogenic emissions and lightning on long-range transport of trace gases and their export from the continent during summers 2002 and 2004, *J. Geophys. Res.*, **116**, D07305, doi:10.1029/2010JD014305.

McCaul, E. W., S. J. Goodman, K. M. LaCasse, and D. J. Cecil, 2009: Forecasting lightning threat using cloud-resolving model simulations, *Wea. Forecasting*, **24**, doi:10.1175/2008WAF2222152.1.

Min, Q.-L., R. Li, B. Lin, E. Joseph, S. Wang, Y. Hu, V. Morris, and F. Chang, 2009: Evidence of mineral dust altering cloud microphysics and precipitation. *Atmos. Chem. Phys.*, **9**, 3223-3231.

Orville, R. E., 2008: Development of the National Lightning Detection Network, *Bull. Amer. Meteor.*, **89**, 180-190, doi:10.1175/BAMS-89-2-180.

Ott, L. E., K. E. Pickering, G. L. Stenchikov, H. Huntrieser, and U. Schumann, 2007: Effects of lightning NO_x production during the 21 July European Lightning Nitrogen Oxides Project storm studied with a three-dimensional cloud-scale chemical transport model, *J. Geophys. Res.*, **112**, D05307, doi:10.1029/2006JD007365.

Ott, L. E., K. E. Pickering, G. L. Stenchikov, D. J. Allen, A. J. DeCaria, B. Ridley, R.-F. Lin, S. Lang, and W.-K. Tao, 2010: Production of lightning NOx and its vertical distribution calculated from three-dimensional cloud-scale chemical transport model simulations, *J. Geophys. Res.*, **115**, D04301, doi:10.1029/2009JD011880.

Petersen, W. A., H. J. Christian, and S. A. Rutledge, 2005: TRMM observations of the global relationship between ice water content and lightning, *Geophys. Res. Lett.*, **32**, L14819, doi:10.1029/2005GL023236.

Pickering, K. E., Y. Wang, W.-K. Tao, C. Price, and J.-F. Müller, 1998: Vertical distribution of lightning NO_x for use in regional and global chemical transport models, *J. Geophys. Res.*, **103**, 31203-31216.

Price, C., and D. Rind, 1992: A simple lightning parameterization for calculating global lightning distributions, *J. Geophys. Res.*, **97**, 9919-9933, doi:10.1029/92JD00719.

Price, C., and D. Rind, 1993: What determines the cloud-to-ground lightning fraction in thunderstorms?, *Geophys. Res. Lett.*, **20**, 463-466.

Ridley, B. A., J. E. Dye, J. G. Walega, J. Zheng, F. E. Grahek, and W. Rison, 1996: On the production of active nitrogen by thunderstorms over New Mexico, *J. Geophys. Res.*, **101**, doi:10.1029/96JD01706.

Schumann, U., and H. Huntrieser, 2007: The global lightning-induced nitrogen oxides source, *Atmos. Chem. Phys.*, **7**, doi:10.5194/acp-7-3823-2007.

Stano, G. T., H. E. Fuelberg, and W. P. Roeder, 2010: Developing empirical lightning cessation forecast guidance for the Cape Canaveral Air Force Station and Kennedy Space Center, *J. Geophys. Res.*, **115**, doi:10.1029/2009JD013034.

Vaisala National Lightning Detection Network: http://www.vaisala.com/en/products/thunderstormandlightningdetectionsystems/Pages/NLDN.aspx, last access: 22 Feb 2014.

Zhang, R., N. T. Sanger, R. E. Orville, X. Tie, W. Randel, and E. R. Williams, 2000: Enhanced NO_x by lightning in the upper troposphere and lower stratosphere inferred from the UARS global NO_2 measurements, *Geophys. Res. Lett.*, **27**, doi:10.1029/1999GL010903.

Zhang, R., X. Tie, and D. W. Bond, 2003:Impacts of anthropogenic and natural NO_x sources over the U.S. on tropospheric chemistry, *PNAS*, **100**, doi:10.1073/pnas.252763799.

Ziegler, C.L., and D.R. MacGorman, 1994: Observed lightning morphology relative to modeled space charge and electric field distributions in a tornadic storm. *J. Atmos. Sci.*, *51*, 833-851.

Table 1. Six flash rate parameterization schemes (FRPSs) incorporated into cloud-resolved-model simulations. Vertical velocity and maximum vertical velocity are represented by w and w_{max}, respectively. H represents the cloud top height at the altitude of 20 dBZ, w_5 represents the updraft volume within the 5 m s^{-1} vertical velocity contour, IWP represents the ice water path, p_m represents the precipitation ice mass, f_p and f_{np} represent the ice mass flux product of precipitating and non-precipitating ice, respectively. The upward flux (F_1) is evaluated at the -15°C level in the mixed-phase region (m), where f is the functional relationship and q_g is the graupel mixing ratio. The vertical integration of graupel (q_g), snow (q_s) and ice (q_i) mixing ratios is performed in each model grid column (dz), where ρ is the local air density and h represents the functional relationship. The blended solution involves weighted contributions, r_1 and r_2, from F_1 and F_2, respectively.

Type of FRPS	Equation (flashes min^{-1})	Reference
Maximum vertical velocity	$5.0 \times 10^{-6} \times w_{max}^{4.5}$	Price and Rind (1992)
Cloud top height	$3.44 \times 10^{-5} H^{4.9}$	Price and Rind (1992)
Updraft volume	$6.75 \times 10^{-11} w_5$ - 13.9	Deierling and Petersen (2008)
Ice water path	$33.33 \times IWP$ - 0.17	Petersen et al. (2005)
Precipitation ice mass	$3.4 \times 10^{-8} p_m$ - 18.1	Deierling et al. (2008)
Ice mass flux product	$9.0 \times 10^{-15} (f_p \times f_{np})$ + 13.4	Deierling et al. (2008)
Upward flux of large precipitating ice	$F_1 = f\left[\left(wq_g\right)_m\right]$	McCaul et al. (2009)
Gridded vertical integral of ice hydrometeors	$F_2 = h\left[\int \rho\left(q_g + q_s + q_i\right)dz\right]$	McCaul et al. (2009)
Blended solution	$F_3 = r_1 F_1 + r_2 F_2$	McCaul et al. (2009)

Table 2. Scaling factors applied to the flash rate parameterization schemes (FRPSs) used in the 29-30 May 2012 Oklahoma case study. The WRF-Chem instantaneous flash rates at 10-min intervals (20:00-02:00 UTC) were compared against the corresponding 1-min periods from the observed NLDN flash rates (21:10-04:10 UTC). A total of 4,468 observed flashes occurred following the methodology of the offline calculation.

Type of FRPS	Total Flashes Prior to Scaling	Scaling Factor
Maximum vertical velocity	3,951	1.1310
Cloud top height	708	6.3138
Updraft volume	21,118	0.2116
Ice water path	4,452	1.0035
Precipitation ice mass	36,745,336	0.0001
Ice mass flux product	164,749	0.0271

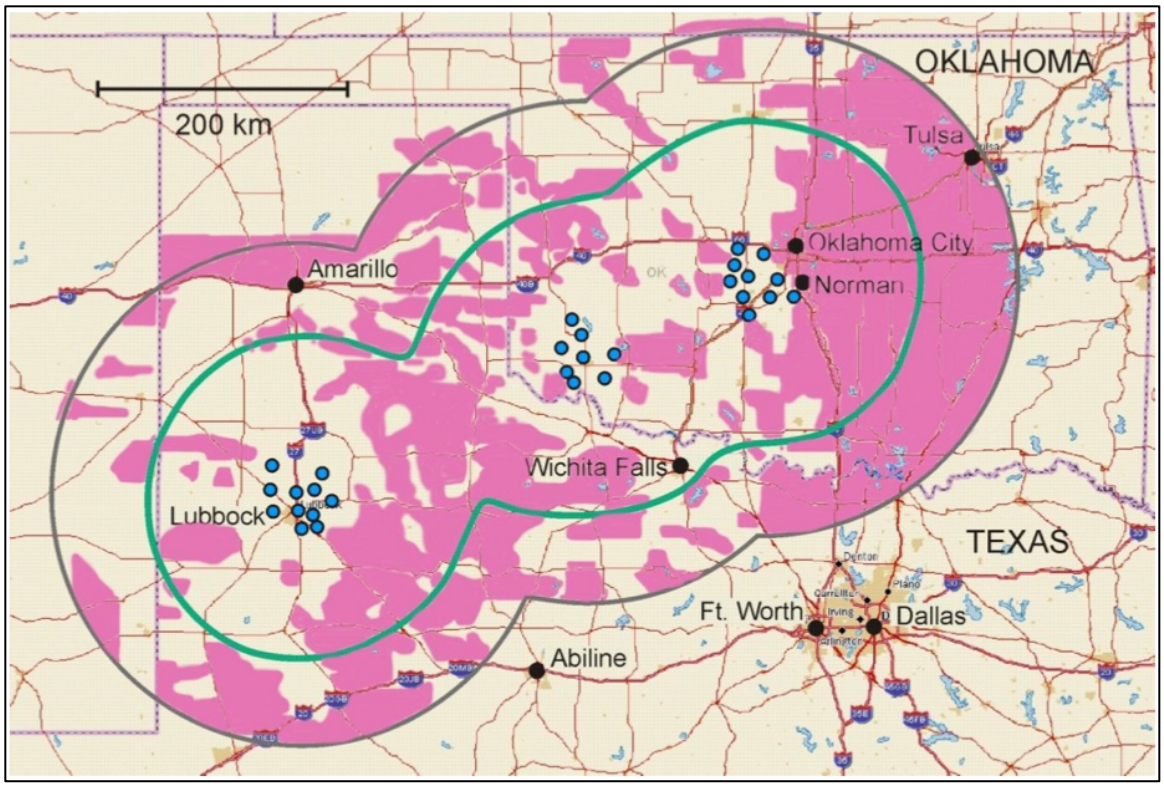

Figure 1. Location of the Oklahoma/west Texas LMA. The blue circles represent the LMA stations. The green outline indicates the extent of the 3D lightning mapping capability. The gray outline indicates the extent of the 2D lightning detection.

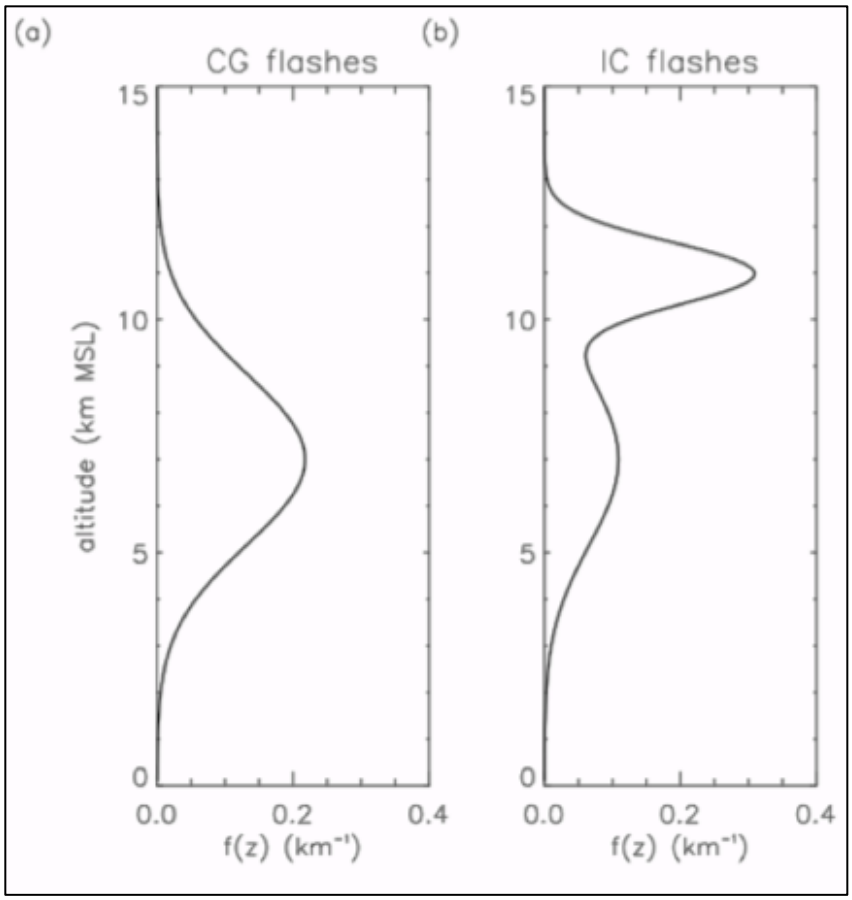

Figure 2. Vertical Gaussian distriubtions of cloud-to-ground (CG) and intracloud (IC) flash channel segments based on DeCaria et al. (2000, 2005). The distributions are representative of midlatitude thunderstorms, where the channels are generally set to maximize at -15°C and -45°C.

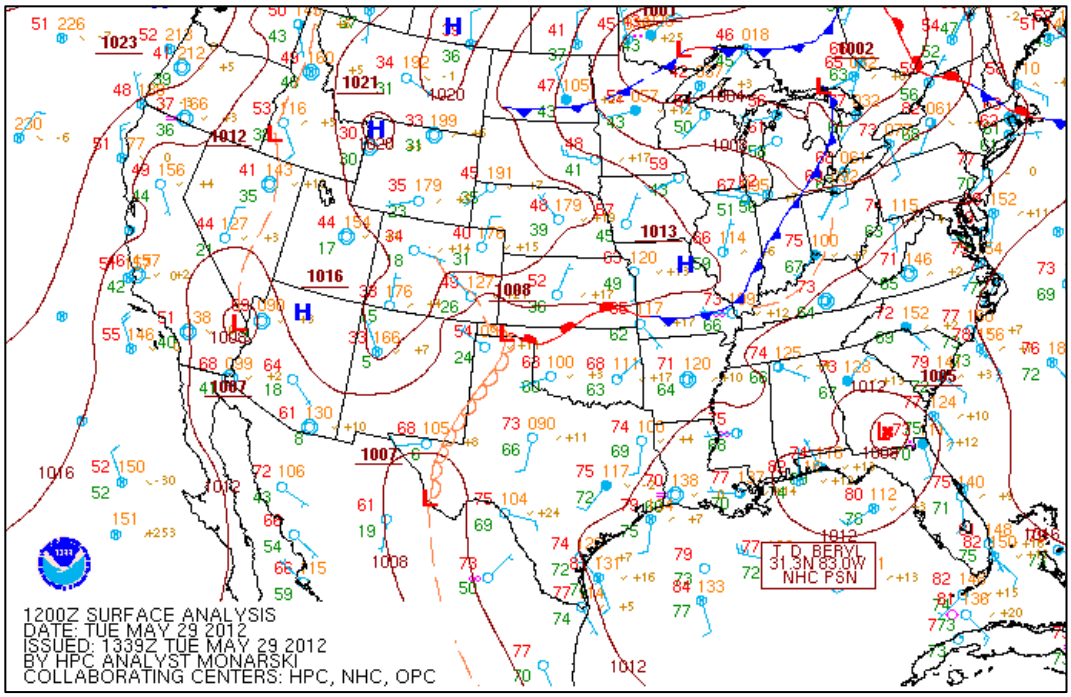

Figure 3. The 12:00 UTC surface analysis from 29 May 2012.

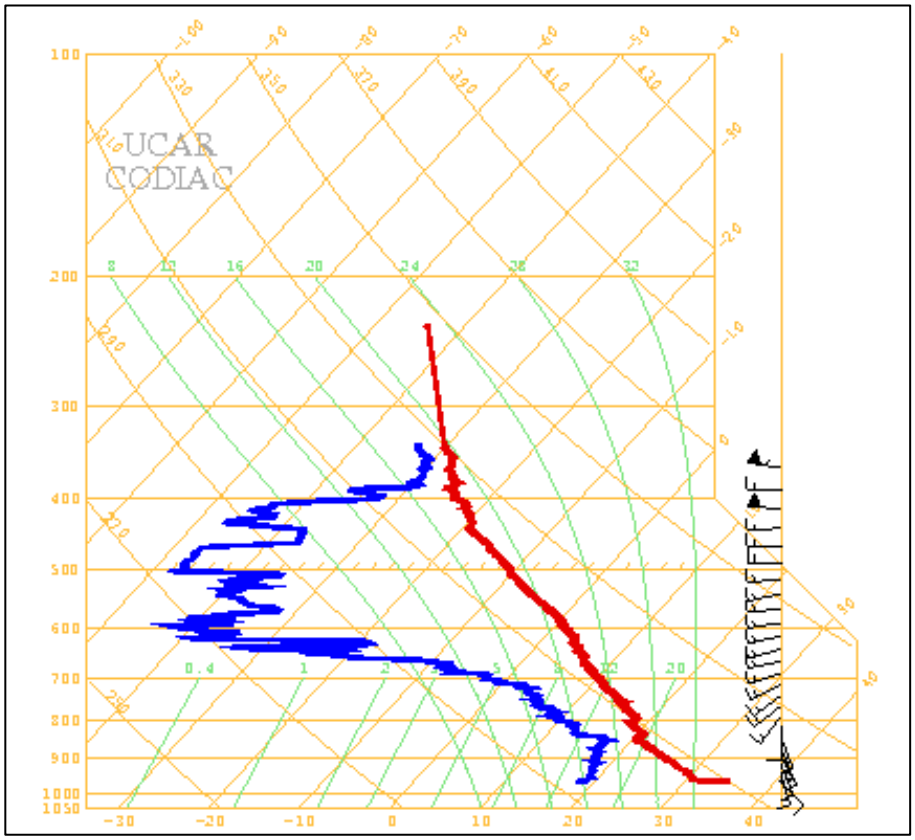

Figure 4. Upper air sounding at 23:00 UTC on 29 May 2012. The NSSL Mobile GPS Advanced Upper-Air Sounding System (MGAUS) was released from 35.85°N, 98.07°W.

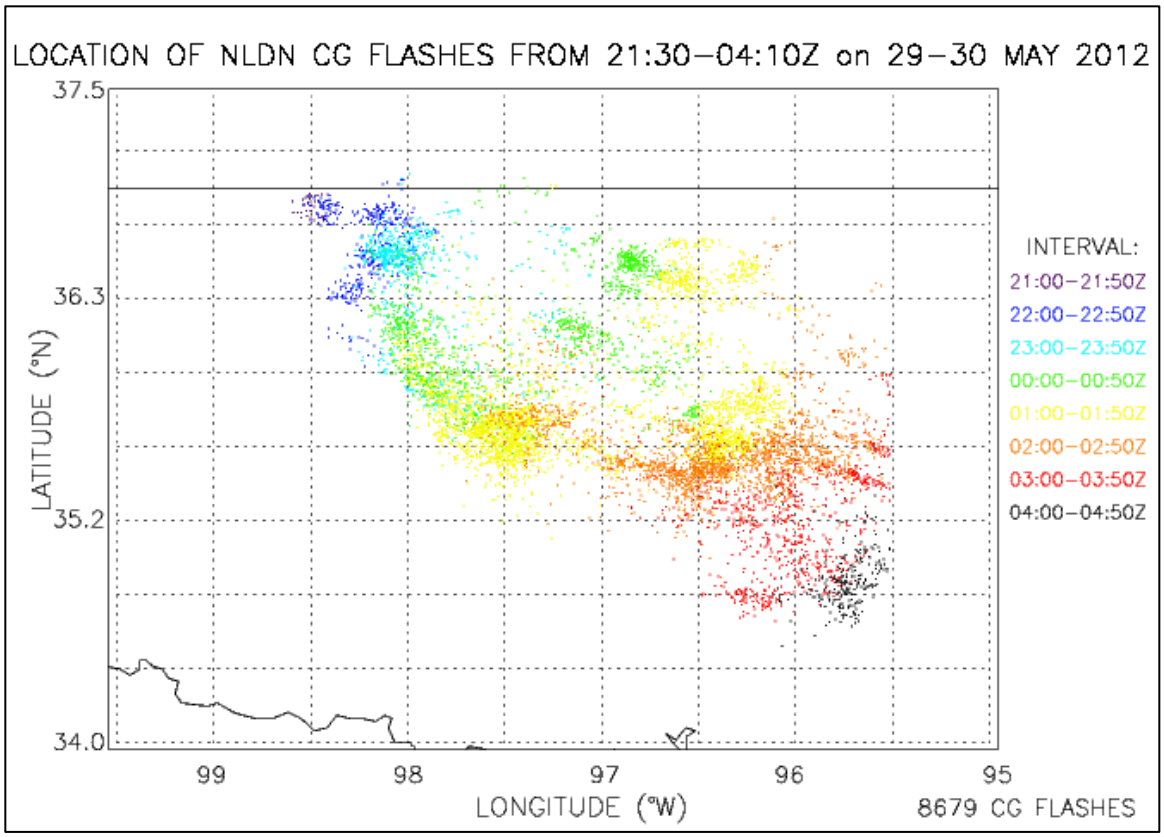

Figure 5. Location of the NLDN CG flashes during the lifetime (21:30-04:10 UTC) of the 29-30 May 2012 Oklahoma thunderstorm. The 1-min CG flash data is color coded by hour.

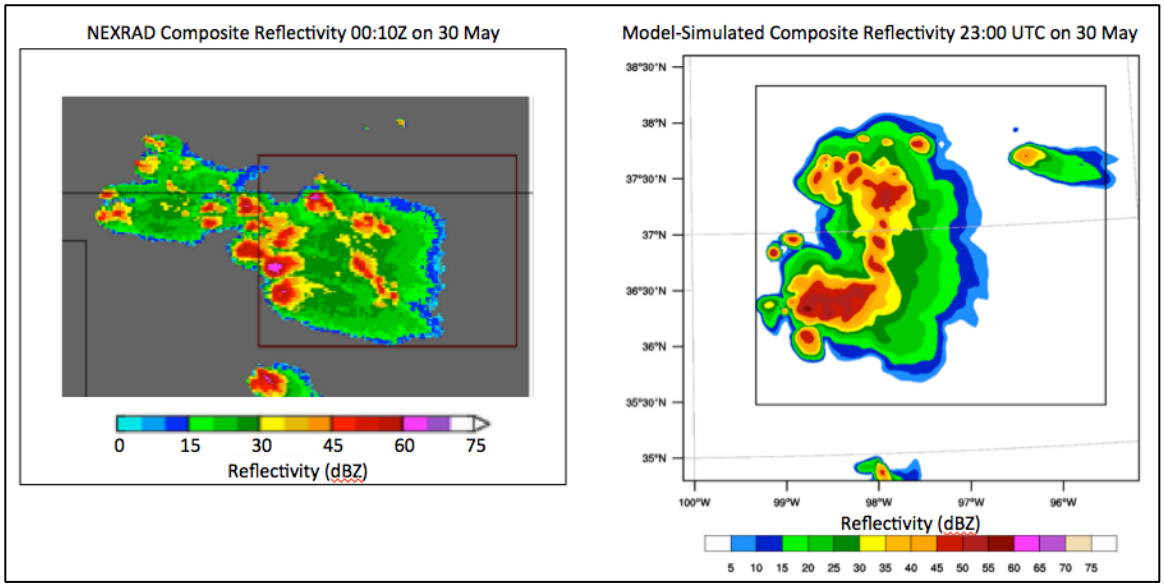

Figure 6. Comparison of the observed composite radar reflectivity at 00:10 UTC (left) to the modeled composite reflectivity at 23:00 UTC (right) for the DC3 29-30 May 2012 Oklahoma thunderstorm. Note the boxes surrounding the observed and model-simulated cells represent the spatial masks applied to each storm at their respective times.

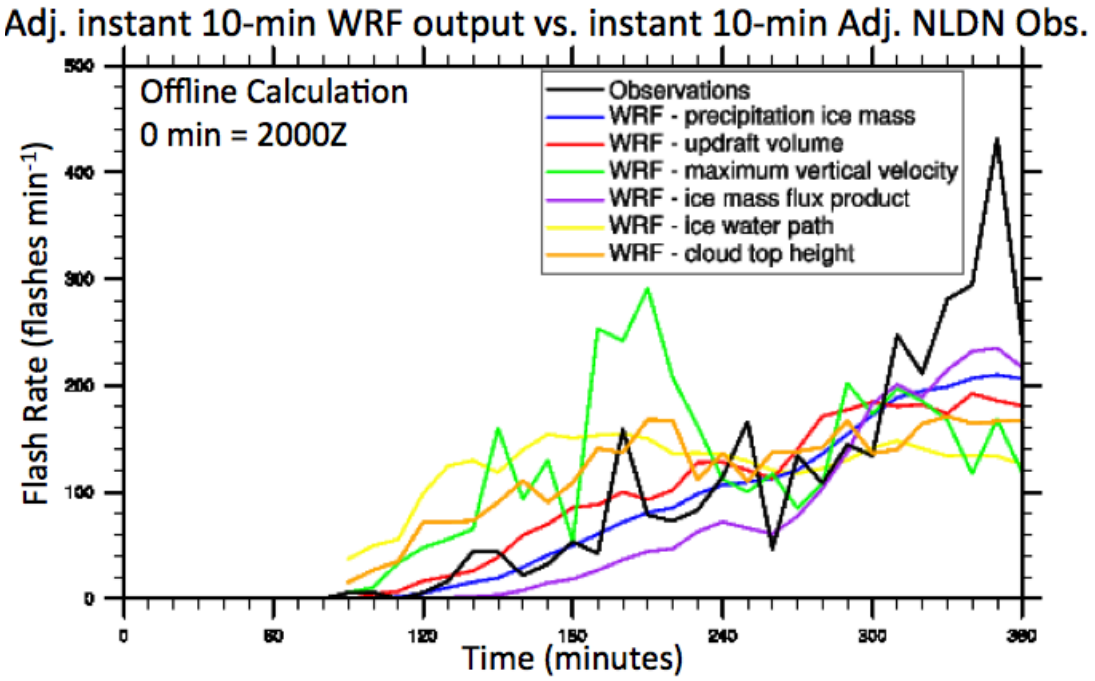

Figure 7. Comparison of the WRF-Chem instantaneous flash rates at 10-min intervals against the corresponding NLDN flash rates at 1-min periods in an offline calculation. Model-simulated flash rates are adjusted 90-min later to coincide with the start of the observed flashes (21:30 UTC) during the DC3 29-30 May 2012 storm.

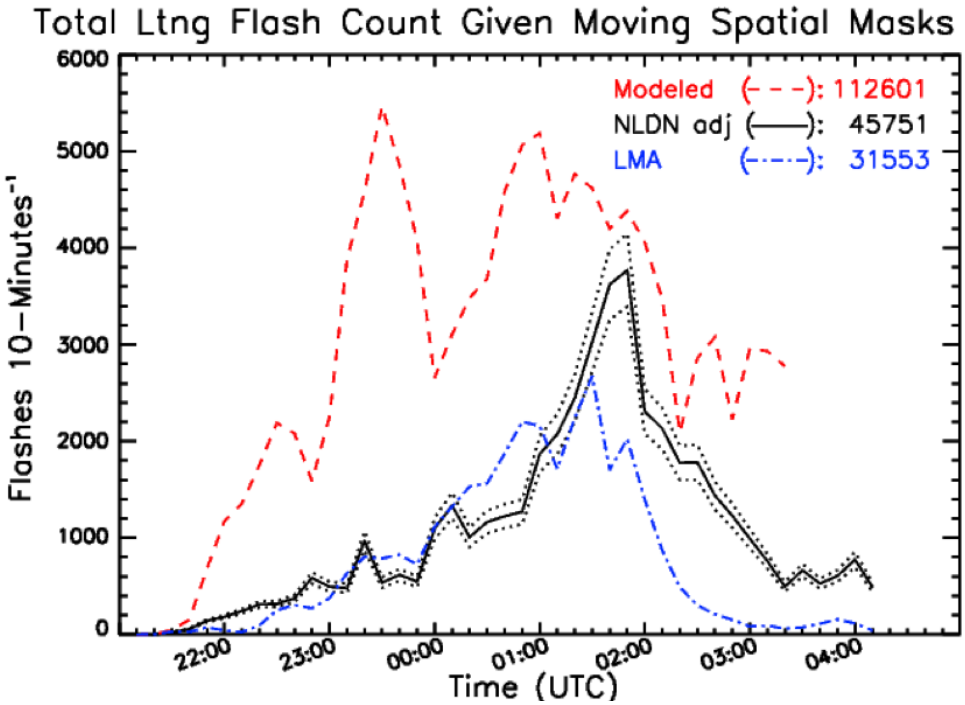

Figure 8. Comparison of the accumulated total (intracloud and cloud-to-ground) flash rates at 10-min intervals from the WRF-Chem and observations during the DC3 29-30 May 2012 storm. Model-simulated flash rates are adjusted 90-min later to coincide with the start of the LMA (21:20 UTC) and NLDN (21:30 UTC) observations.

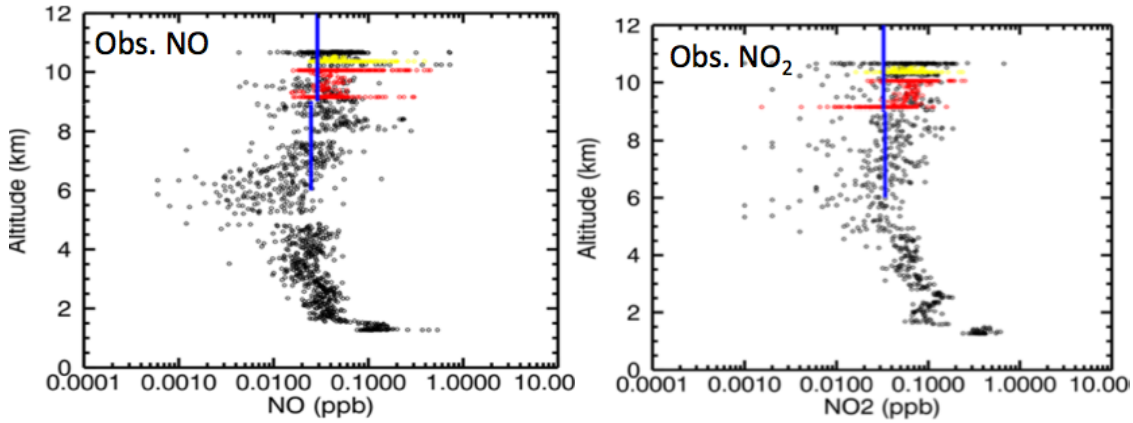

Figure 9. NO and NO_2 mixing ratios observed in cloud-free air by the GV (yellow and red) and DC-8 (black) between 22:15-23:05 UTC and 20:40-21:10 UTC on 29 May 2012, respectively (courtesy of M. Bela). Units are in ppbv.

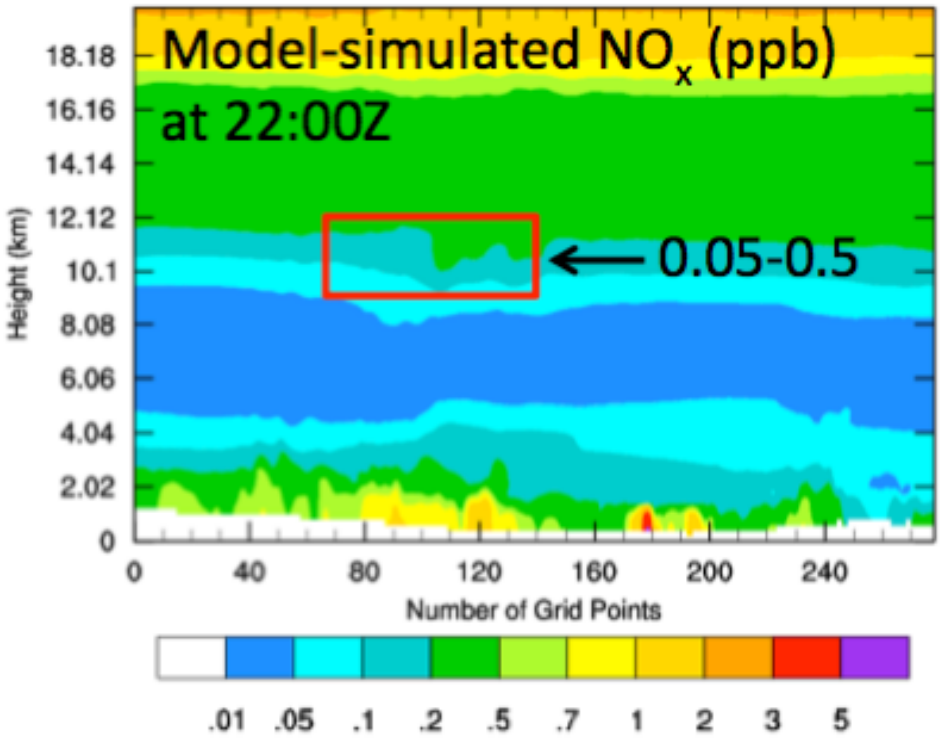

Figure 10. Vertical cross-section of model-simulated NO_x mixing ratios in ppbv. The cross-section is taken south of the model-simulated storm in cloud-free air at 22:00 UTC on 29 May 2012. The red rectangle represents the area from the model simulation used in the NO_x mixing ratio comparison against the aircraft observations.

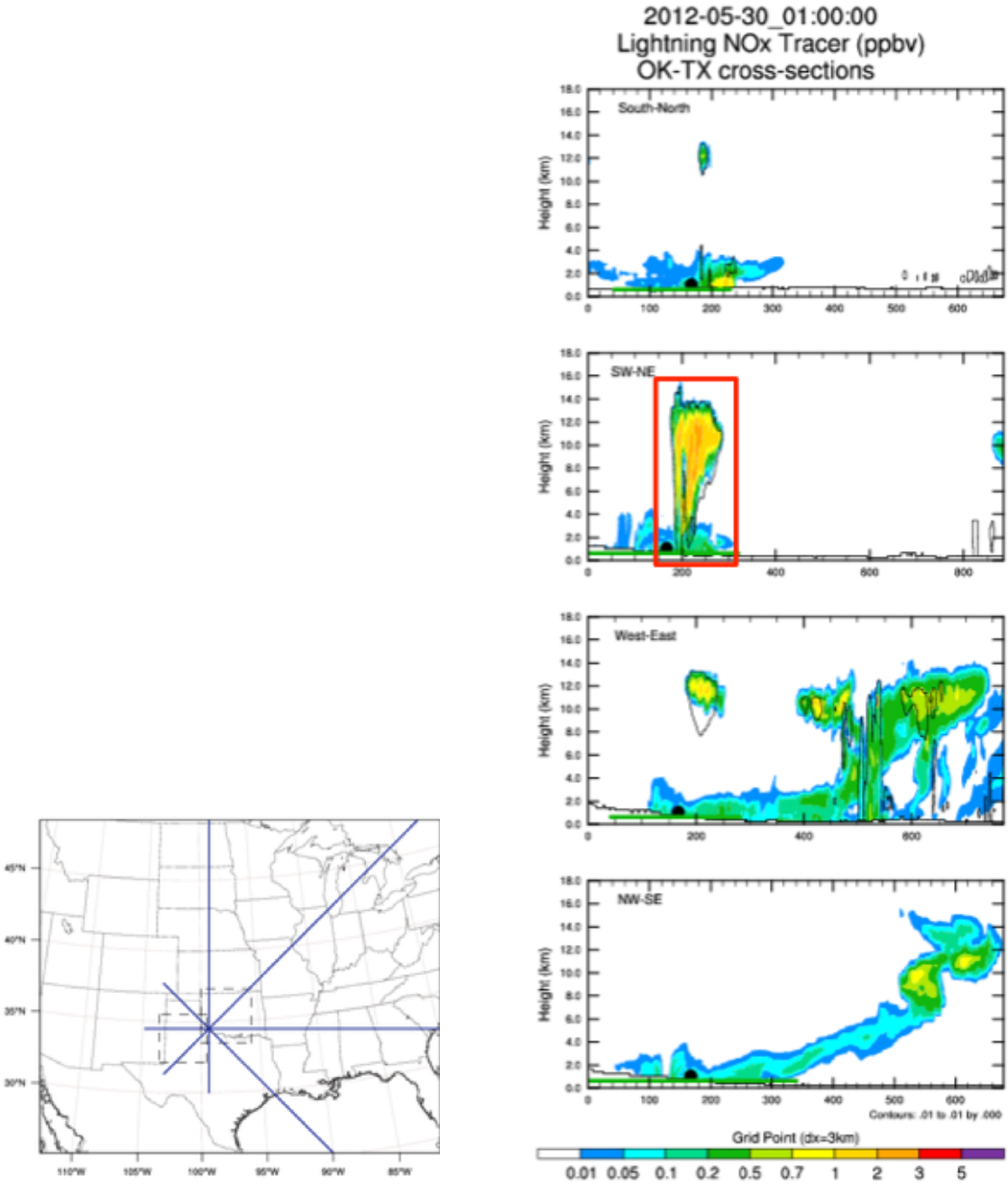

Figure 11. The map on the left indicates the location of the four vertical cross-sections (south-north, southwest-northeast, west-east, and northwest-southeast) taken over the Oklahoma domain. The plots on the right show the LNO_x model forecast along each of the vertical cross-sections at 01:00 UTC on 30 May 2012. The red rectangle represents the convective cell of interest, which was forecast to develop over the Oklahoma domain. Units are in ppbv.